ARTICLE IN PRESS

Available online at www.sciencedirect.com
SCIENCE DIRECT®

Chemical Physics Letters 417 (2005) 200–205

CHEMICAL PHYSICS LETTERS

www.elsevier.com/locate/cplett

Energy dispersive X-ray diffraction and molecular dynamics meet: The structure of liquid pyrrole

Lorenzo Gontrani [a], Fabio Ramondo [b], Ruggero Caminiti [c,*]

[a] *C4T S. C. a r. L., Università di Roma, 'Tor Vergata', V. d. ricerca scientifica, I-00133 Roma, Italy*
[b] *Dipartimento di Chimica, Ingegneria Chimica e Materiali, Università dell'Aquila, Loc. Coppito, I-67100 L'Aquila, Italy*
[c] *Dipartimento di Chimica, Università di Roma, 'La Sapienza', P. le Aldo Moro 5, I-00185 Roma, Italy*

Received 8 July 2005; in final form 4 October 2005

Abstract

In this work, a coupled experimental–theoretical protocol for the study of molecular liquids is reported. Energy dispersive X-ray diffraction results are successfully interpreted with molecular dynamics. Several models, differing for geometry and force field are presented; their behavior in reproducing experimental data is discussed.

1. Introduction

Pyrrole (C_4H_5N) is one of the simplest etheroaromatic molecules, being made up of a single five-membered ring. In spite of its apparent simplicity, the pyrrole moiety is one of the most important structural motifs in chemistry, since it spans both the 'organic' [1] and the 'inorganic' world. As a fundamental subunit of porphyrins, in fact, it is present both in the former (e.g. heme, chlorophylls) and in the latter (e.g. metallophtalocyanines); moreover, the importance of pyrrole polymers has long been recognized, since they show a remarkable electric conductivity [2–5]. The outstanding importance of pyrrole structure can be attributed to its facility to polymerize and to form N–H $\cdots$ π hydrogen bonds with near molecules. Due to the widespread interest in pyrrole chemistry, several structural studies have been performed so far, both with experimental techniques and with theoretical methods. Among all the Letters, we cite the first studies in gas phase with microwave spectroscopy and electron diffraction of the monomer [6] and dimer [7,8], quantomechanical calculations [9], vibrational spectroscopy in inert matrix and solid state [10], and crystal structure determination [11]. All the studies reveal the molecule great tendency to form aggregates, approximately T-shaped. Few experimental studies (see e.g. [12]) on liquid pyrrole, instead, have been performed so far; unfortunately, none of them is of structural type. Theoretical studies of liquid pyrrole, furan, diazoles and oxazoles have been reported [13]. In the present work, we report the first study of the neat liquid using X-ray diffraction, a technique that provides a very good structural insight. Several examples of the application of angle dispersion X-ray diffraction to pure liquids and solutions of metal ions can be found in the literature (see e.g. [14–19]). In a few cases, experimental data have been interpreted successfully with theoretical methods, such as Monte-Carlo or molecular dynamics simulations [20–23]. Here, energy dispersive X-ray diffraction (EDXD) has been used. Use of this technique has several advantages when compared with traditional ADXD (angular dispersive) [24–29]: for instance, diffraction spectra can be collected much faster and using only few reflection angles, though q ranges obtainable are equal to or larger than those of traditional diffraction (see Section 2); moreover, a variety of experimental equipment is available.

* Corresponding author. Fax: +39 06490631.
E-mail address: r.caminiti@caspur.it (R. Caminiti).

0009-2614/$ - see front matter © 2005 Published by Elsevier B.V.
doi:10.1016/j.cplett.2005.10.021

2. Experimental

2.1. Sample preparation

Liquid pyrrole (melting point: −23 °C, boiling point: 131 °C, density = 0.967 kg L^{-1}) was purchased from Aldrich.

2.2. X-ray diffraction: data treatment

We performed our experiments using the non-commercial energy-scanning diffractometer built in the Department of Chemistry, Rome University. Detailed description of both instrument and technique can be found elsewhere [24–27]. Transmission geometry has been employed. White Bremsstrahlung component of the radiation emitted by a tungsten tube working at 45 kV and 35 mA was used. Scattered intensities for the two samples and for the empty cell were measured at seven different angles (26.0, 15.5, 8.0, 3.5, 2.0, 1.0 and 0.5°). This choice allowed us to cover a wide range of the scattering variable q, namely between 0.12 and 17 $Å^{-1}$. The measuring time was set so as to obtain a minimum of 300 000 counts per experimental point for $q < 5\ Å^{-1}$ and 600 000 counts for $q \geqslant 5Å^{-1}$. This large amount of counts can be achieved in a limited period of time with EDXD (with respect to ADXD), resulting in a significant improvement of signal-to-noise ratio at high angles. The expression for q is:

$$q = \frac{4\pi \sin\theta}{\lambda} = E \cdot 1.014 \sin\theta, \tag{1}$$

when E is expressed in keV and q in $Å^{-1}$. The primary beam intensity $I_0(E)$ was measured directly, by reducing the tube current to 10 mA at zero scattering angle without the sample. Transmission of the samples was measured under the same conditions. Both quantities are needed to carry out necessary corrections to observed scattered intensities. After correction of experimental data for escape peak suppression [30], the various angular data were combined and the re-scaled intensity, in electron units (e.u.), was normalized to a stoichiometric unit of volume containing one N atom. Such correction was performed using our program DIF1, purposely written. Detailed description of procedures and formulae used can be found in [30–32]. The 'static' structure function $I(q)$ was constructed according to the formula

$$I(q) = I_{\text{e.u.}} - \sum_{i=1}^{n} x_i f_i^2, \tag{2}$$

where f_i are the atomic scattering factors, x_i are the number concentrations of i-type atoms in the stoichiometric unit and $I_{\text{e.u.}}$ is the observed intensity in electron units. Fourier transformation of $I(q)$ led to radial distribution functions (RDF)

$$D(r) = 4\pi r^2 \rho_0 + \frac{2r}{\pi} \int_0^{q_{\max}} qI(q)M(q) \sin(rq)\ \mathrm{d}q. \tag{3}$$

In this equation, ρ_0 is the bulk number density of stoichiometric units and

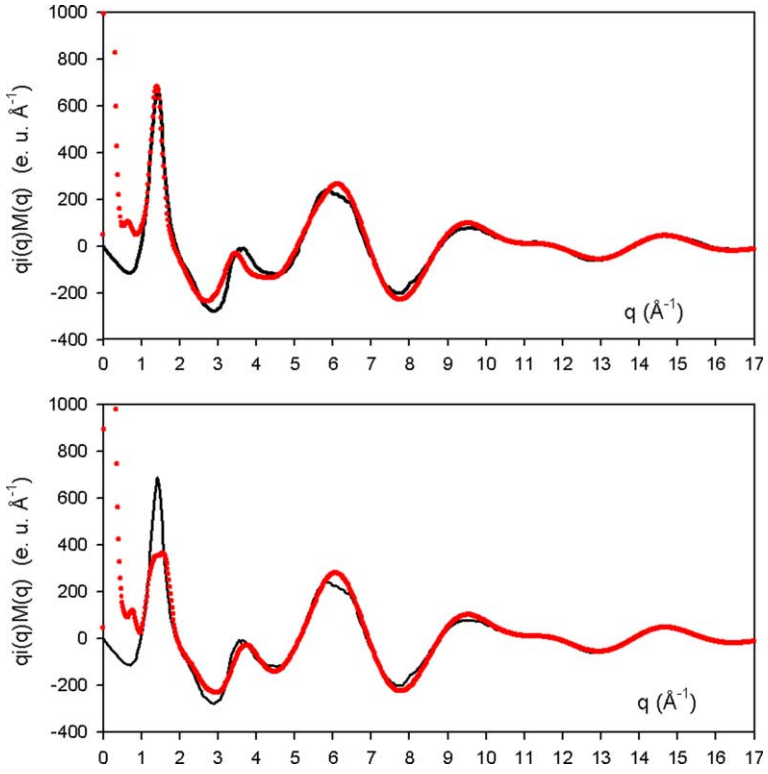

Fig. 1. Experimental structure function – black versus theoretical functions – red. Top: MMFF94X; bottom: GAFF. (For interpretation of the references in colour to this figure legend, the reader is referred to the Web version of this article.)

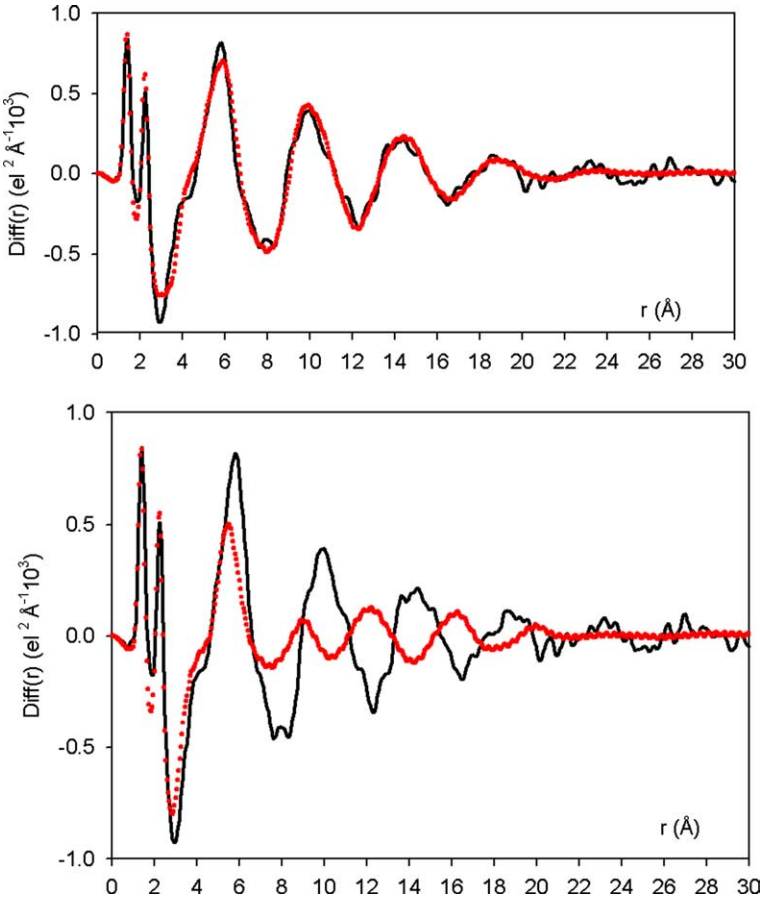

Fig. 2. Radial distribution functions (Diff(r)) – black versus theoretical functions – red. Top: MMFF94X; bottom: GAFF. (For interpretation of the references in colour to this figure legend, the reader is referred to the Web version of this article.)

$$M(q) = \frac{f_N^2(0)}{f_N^2(q)} \exp(-0.01q^2), \tag{4}$$

is the sharpening factor. We used the value of 17 Å^{-1} as the upper limit of integration. The measured functions for liquid pyrrole at 25 °C are reported (black) in Fig. 1 (structure function in the form $qI(q)M(q)$) and in Fig. 2 (RDF – in the form $\mathrm{Diff}(r) = D(r) - 4\pi r^2\rho_0$), both versus the two respective model functions (in red: MMFF94x/top; GAFF/bottom; see the following section). As it can be seen from the pictures, pyrrole is a moderately ordered liquid. In fact, the $I(q)$ function (in 'reciprocal space') shows a principal peak (at 1.5 Å^{-1}, approximately), followed by four less intense peaks. The first peak is attributable to long-range interactions. This 'order' can be better appreciated in the Fourier transform of $I(q)$ ('direct space'). The Diff(r) curve shows, in fact, at least four well-resolved peaks besides the first two ones (intramolecular interactions) at 6, 10, 15 and 19 Å; two less intense peaks can still be noticed at 23 and 27 Å. No type of 'structure' appears further on.

3. Results and discussion

The features inferred from the analysis of experimental curves were used to build a structural model the structure function and radial distribution function of which best fitted the experimental data. Theoretical peaks were calculated by Fourier transformation of a model structure function obtained by the Debye equation for pairs of interactions:

$$i_{mn}(q) = \sum f_m f_n \frac{\sin(r_{mn}q)}{r_{mn}q} \exp\left(-\frac{1}{2}\sigma_{mn}^2 q^2\right), \tag{5}$$

using the same sharpening factor, the same q_{max} value as for experimental data and assuming σ_{mn} to be the root-mean-square (r.m.s.) variation in the interatomic distance r_{mn}. The same σ value is generally attributed to distances falling within predefined ranges (see, for instance, [24]). In this work, instead (see later in the text), we used the value of zero for all σ_{mn}, since our model is derived from molecular dynamics, thus already incorporating thermal uncertainties (which are responsible for peak broadening).

The Fourier transform process requires extrapolation to zero of the model structure function to account for long distance interactions (uniform distribution, the so-called 'continuum'). We decided to replace model data below 1.1 Å^{-1} with experimental ones, since the proposed equations for the continuum have no direct physical meaning. Two distinct interpreting models were constructed employing the all-atom force fields MMFF94X (Merck Force Field) [33] and the General AMBER force field (GAFF)

[34]. (See the references and MOE manual [35] for detailed force field functional form; MMFF94X parameters are reported in Table 1 of Supplementary Materials.) The calculation proceeded in the following way:

- The pyrrole molecule ('cleaned' by a simple builder) was first replicated in three dimensions, using the routine 'solvatebox' of leap (AMBER) [36]. A 'pseudo-crystal' of 39 molecules was obtained.
- The system was then processed with the energetic modules of MOE [35] in the case of MMFF94X and with AMBER utilities (antechamber, tleap [36]) for GAFF; atom types were assigned;
- AM1 Point charges were calculated with MOPAC software [37] in the GAFF case, while no calculation was needed for MMFF94X model, since charges are automatically assigned by the software in this case.
- The structure was first minimized up to a gradient of 0.05 and then simulated with molecular dynamics (MD). A trajectory of 1100 ps (100 ps heating + 1000 ps production) in NVT *ensemble* was produced, with coordinates dumping every picosecond (1100 frames in total). Both values are enough to get a good agreement with experimental data. No periodic boundary conditions were applied, and SHAKE algorithm was used throughout all the simulation.

In Fig. 3, the structure functions of starting 'pseudo-crystal' (top, red) and of minimized structure obtained with MMFF94X model (bottom, red) are plotted together with experimental $I(q)$ (black). The starting structure can be seen in Fig. 4, while in Fig. 5 a typical MD frame is shown. We calculated the Debye structure functions for every configuration saved. In the case of molecular dynamics trajectories, all 1100 sampled snapshots were averaged, thus obtaining a single function. As it can be noticed, the first system (Fig. 3 top and 4) produces a $I(q)$ with very sharp peaks (it has a too high 'degree of crystallinity' for a liquid); the minimization (3, bottom) leads to a significant amount of disorder, but only molecular dynamics (which takes into account thermal motions) is able to reproduce the correct peak shapes and intensities (Fig. 1) in $I(q)$; this fact is even clearer when passing to 'direct space' (Fig. 2). In both pictures, the theoretical curves for both MD trajectories (red) are compared with experimental ones (black). It can be seen that the model built with MMFF94X force field (top) shows a much better agreement than that of GAFF model (bottom), with very good reproduction of peak positions, shapes and intensities. The model extends up to about 25 Å; therefore, it cannot fit experimental data beyond that limit. A slight increase of the number of molecules would probably lead to fitting of the entire curve. In a visual inspection of GAFF models, the molecules appeared to be too close to each other, thus giving an 'empty' principal peak in structure function, which leads to too short distance peaks in RDF (Fig. 2, red). The MMFF94X model can be described as a complex aggregate of dimers oscillating between T-shape and stacked form, with an average population of 50% each.

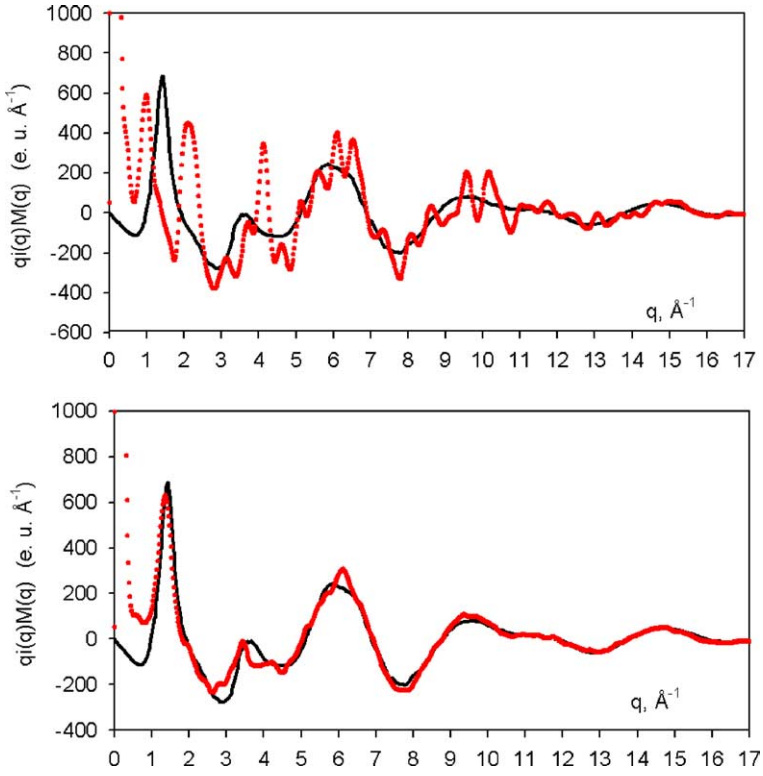

Fig. 3. Experimental structure function – black versus theoretical functions – red. Top: starting structure; bottom: MMFF94X minimized structure. (For interpretation of the references in colour to this figure legend, the reader is referred to the Web version of this article.)

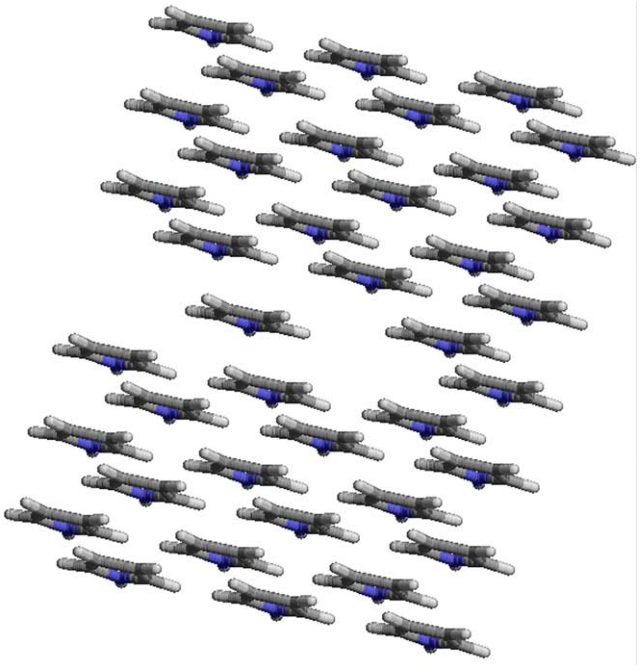

Fig. 4. Starting structure.

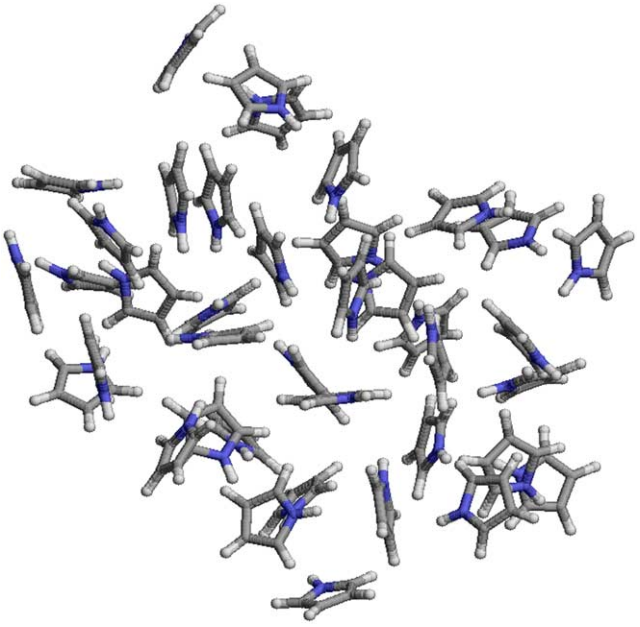

Fig. 5. Average mean structure of MMFF94X trajectory.

4. Conclusion

In this work, we report an example of a coupled experimental–theoretical method to study liquid structure. It combines energy dispersive X-ray diffraction, which is a very powerful and versatile technique, with molecular dynamics, likely the most widely used theoretical method in all fields of chemical, biological and physical research. The method was applied to the study of pyrrole, a moderately ordered liquid, and led to very good agreement between theory and experiment. The best model was built using MMFF94X, a general-purpose all-atom force field; this force field is complete and can readily be applied to other molecular liquids, as well as to other partially ordered systems. Some experiments on amorphous and low melting molecular solids at various temperatures are being performed in our lab.

Acknowledgments

We wish to thank CASPUR (Centro di Applicazioni di Supercalcolo per Università e Ricerca) for technical support, Dr. C. Sadun and Dr. O. Incani for help and stimulating discussion.

Appendix A. Supplementary data

Supplementary data associated with this article can be found, in the online version, at doi:10.1016/j.cplett.2005.10.021.

References

[1] H. Fischer, H. Orth, Akademische Verlag: Die Chemie des Pyrrols, vol. I, (1934, 1937, 1940), Leipzig.
[2] B.E. Kohler, in: H. Kuzmany, M. Mehring, S. Roth (Eds.), Electronic Properties of Polymers and Related Compounds, Springer, Berlin, 1985, p. 100.
[3] J. Wang, K. Neoh, E. Kang, Thin Solid Films 446 (2004) 205.
[4] S. Kim, K. Oh, J. Bahk, J. Appl. Polym. Sci. 91 (2004) 4064.
[5] R. Kanakaraju, P. Kolandaivel, Int. J. Mol. Sci. 3 (2002) 777.
[6] W. Wilcox, J. Goldstein, J. Chem. Phys. 20 (1952) 1656.
[7] B. Bak, D. Christensen, L. Hansen, J. Rastrup-Andersen, J. Chem. Phys. 24 (1956) 720.
[8] L. Nyagaard, J. Nielsen, J. Kirchheiner, G. Maltesen, J. Rastrup-Andersen, G. Soerensen, J. Mol. Struct. 3 (1969) 491.
[9] M. Kofranek, Tomáš Kovář, A. Karpfen, H. Lischka, J. Chem. Phys. 96 (6) (1992) 4465.
[10] A. Gómez-Zavaglia, R. Fausto, J. Phys. Chem. A 108 (2004) 6953.
[11] R. Goddard, O. Heinemann, C. Krüger, Acta Crystallogr. C53 (1997) 1846.
[12] A.E. Lutskii, V.N. Solon'ko, E.I. Goncharova, Primenenie Ul'traakustiki k Issledovaniyu Veshchestva 20 (1964) 29.
[13] N.A. Macdonald, W.L. Jorgensen, J. Phys. Chem. B 102 (41) (1998) 8049.
[14] A.H. Narten, S. Lindenbaum, J. Chem. Phys. 51 (1969) 1108.
[15] A.H. Narten, H.A. Levy, J. Chem. Phys. 55 (1971) 2263.
[16] R. Caminiti, J. Chem. Phys. 77 (1982) 5682.
[17] R. Caminiti, Chem. Phys. Lett. 96 (1983) 390.
[18] R. Caminiti, P. Cucca, Chem. Phys. Lett. 108 (1984) 51.
[19] R. Caminiti, C. Sadun, M. Carbone, J. Mol. Liq. 75 (1998) 149.
[20] J.C. Soetens, C. Millot, B. Maigret, I. Bakò, J. Mol. Liq. 92 (2001) 201.
[21] G. Hura, D. Russo, R.M. Glaeser, T. Head-Gordon, M. Krack, M. Parrinello, Phys. Chem. Chem. Phys. 5 (2003) 1981.
[22] I. Akiyama, M. Ogawa, K. Takase, T. Takamuku, T. Yamaguchi, N. Othori, J. Sol. Chem. 33 (2004) 797.
[23] T. Radnai, T. Megyes, I. Bakò, T. Kosztolànyi, G. Pàlinkàs, H. Ohtaki, J. Mol. Liq. 110 (2004) 123.
[24] L. Gontrani, R. Caminiti, L. Bencivenni, C. Sadun, Chem. Phys. Lett. 301 (1–2) (1999) 131.
[25] R. Caminiti, V. Rossi Albertini, Int. Rev. Phys. Chem. 18 (2) (1999) 263.

[26] R. Caminiti, M. Carbone, S. Panero, C. Sadun, J. Phys. Chem. 103 (47) (1999) 10348.
[27] D. Atzei, T. Ferri, C. Sadun, P. Sangiorgio, R. Caminiti, J. Am. Chem. Soc. 123 (11) (2001) 2552.
[28] P. Ballirano, R. Caminiti, J. Appl. Cryst. 34 (2001) 757.
[29] S. Meloni, A. Pieretti, L. Bencivenni, V. Rossi Albertini, C. Sadun, R. Caminiti, Comp. Mater. Sci. 20 (3–4) (2001) 407.
[30] Y. Murata, K. Nishikawa, Bull. Chem. Soc. Jpn. 51 (2) (1978) 411.
[31] K. Nishikawa, T. Iijima, Bull. Chem. Soc. Jpn. 57 (1984) 1750.
[32] G. Fritsch, C.N.J. Wagner, Z. Phys. B – Condens. Matter 62 (1986) 189.
[33] T.A. Halgren, J. Comput. Chem. 17 (1996) 587.
[34] J. Wang, R.M. Wolf, J.W. Caldwell, P.A. Kollamn, D.A. Case, J. Comput. Chem. 25 (2004) 1157.
[35] ©1997–2005 Chemical Computing Group Inc. All rights reserved.
[36] D.A. Case, D.A. Pearlman, J.W. Caldwell, T.E. Cheatham III, J. Wang, W.S. Ross, C.L. Simmerling, T.A. Darden, K.M. Merz, R.V. Stanton, A.L. Cheng, J.J. Vincent, M. Crow-ley, V. Tsui, H. Gohlke, R.J. Radmer, Y. Duan, J. Pitera, I. Massova, G.L. Seibel, U.C. Singh, P.K. Weiner, P.A. Kollman, AMBER 7, University of California, San Francisco, 2002.
[37] J.J.P. Stewart, Quant. Chem. Prog. Exch. 10 (1990) 86.